Supporting Information

Novel Metallated Imidazole Phthalocyanines: Synthesis, Ultrafast Excited State Carrier Dynamics and Multiphoton Absorption Properties

Md Soif Ahmed,[a] Kalavala Shivaprakash Srivishnu,[b,c] Chinmoy Biswas,[a] Prabhakar Chetti,[d] Venugopal Rao Soma,[e] Lingamallu Giribabu,[b,c]* Sai Santosh Kumar Raavi[a, f]*

[a] *Ultrafast Photophysics and Photonics Laboratory, Department of Physics, Indian Institute of Technology Hyderabad, Kandi 502285, Telangana, India*

[b] *Polymers& Functional Materials Division, CSIR-Indian Institute of Chemical Technology, Tarnaka, Hyderabad-500007, India*

[c] *Academy of Scientific and Innovative Research (AcSIR), Ghaziabad- 201002, India*

[d] *Department of Chemistry, National Institute of Technology, Kurukshetra 136119, India*

[e] *Advanced Centre of Research in High Energy Materials (ACRHEM), DRDO Industry Academia – Centre of Excellence (DIA-COE), University of Hyderabad, Hyderabad 500046, Telangana, India*

[f] *Department of Climate Change, Indian Institute of Technology Hyderabad, Kandi 502285, Telangana, India*

Corresponding author's e-mail addresses: sskraavi@phy.iith.ac.in and giribabu@iict.res.in

Absorption and photoluminescence

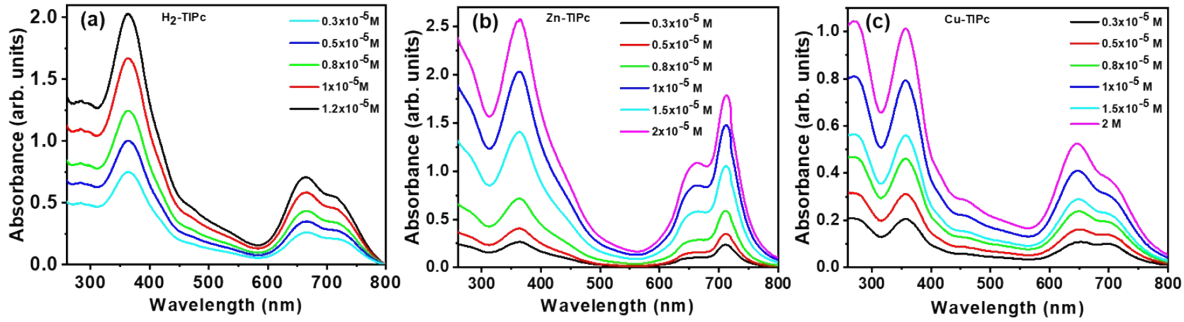

Fig. S1. Absorption spectral changes of (a) H_2-TIPc, (b) Zn-TIPc and (c) Cu-TIPc in DCM at different concentrations.

Time-resolved photoluminescence

Excitation laser wavelength: ~ 640 nm.

TRPL is measured at emission wavelength of 720 nm.

Table S1

PL decay parameters of the samples obtained by TCSPC. Residuals (χ^2), bi-exponential decay time fit parameters τ_1 and τ_2 with respective % (Rel. %) are presented here.

Sample	$\tau_1(ns)$	**Rel. %**	$\tau_2(ns)$	**Rel. %**	χ^2
H_2-TIPc	1.88	11.61	**4.97**	88.39	1.06
Zn-TIPc	**2.30**	92.88	5.71	7.12	1.13

Model used to fit the time-resolved photoluminescence (TRPL) using exponential reconvolution with instrument response function (IRF):

Fitting equation: $A + B1\ exp\left(-\frac{t}{\tau_1}\right) + B2\ exp\left(-\frac{t}{\tau_2}\right)$; for bi-exponential decay

Details of TCSPC fitting parameters and values:

- **H_2-TIPc**

Time Calibration : 0.098 ns/ch
Total Experiment Time : 249.25 s

Fit Range (ch) : 107 to 512

Parameter	Value	Std. Dev.	Rel %
τ_1	1.882E-009 s	1.4134E-010 s	
τ_2	4.968E-009 s	4.2755E-011 s	
Shift	2.012E-011 s	4.532E-011 s	
B1	0.037	0.0021	11.61
B2	0.108	0.0025	88.39
A	78.619		
χ^2	1.062		

- **Zn-TIPc**

Time Calibration : 0.098 ns/ch
Total Experiment Time : 147.01 s

Fit Range (ch) : 108 to 512

Parameter	Value	Std. Dev.	Rel %
τ_1	2.304E-009 s	2.4933E-011 s	
τ_2	5.708E-009 s	6.7885E-010 s	
Shift	9.967E-011 s	8.441E-011 s	
B1	0.162	0.0055	92.88
B2	0.005	0.0017	7.12
A	45.218		
χ^2	1.135		

Electrochemical and spectroelectrochemical studies

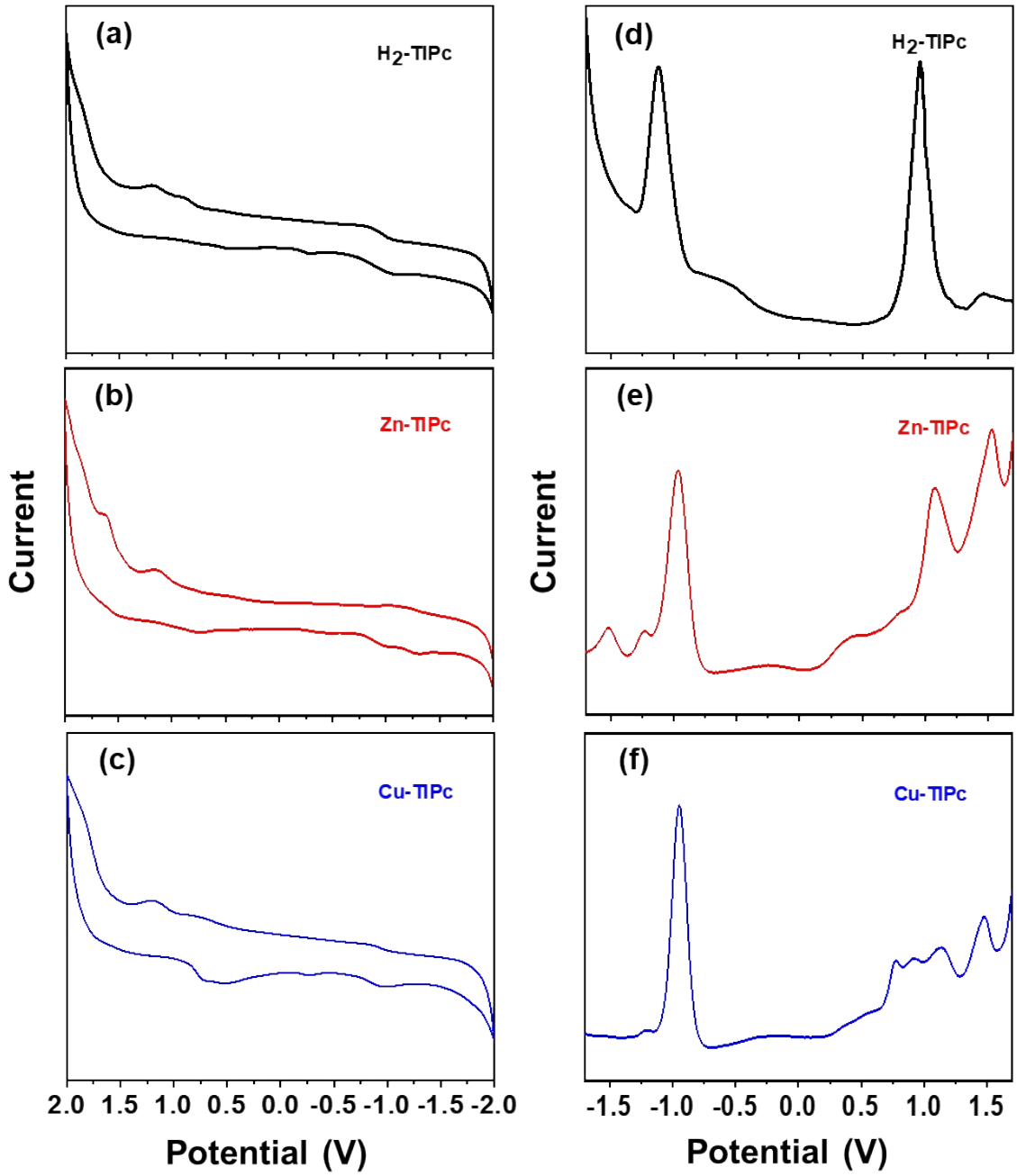

Fig. S2. Cyclic voltammograms of (a) H_2-TIPc, (b) Zn-TIPc and (c) Cu-TIPc; differential pulse voltammetry (DPV) curves of (d) H_2-TIPc, (e) Zn-TIPc and (f) Cu-TIPc.

DFT Studies

Table S2

Ground (S_0) and excited (S_1) state geometries obtained at B3LYP/6-31G (d, p) and TD-B3LYP/6-31G (d, p) in combination with LANL2DZ, respectively.

Molecules	Ground (S_0) Optimized Structure	Excited (S_1) Optimized Structure
H_2-TIPc	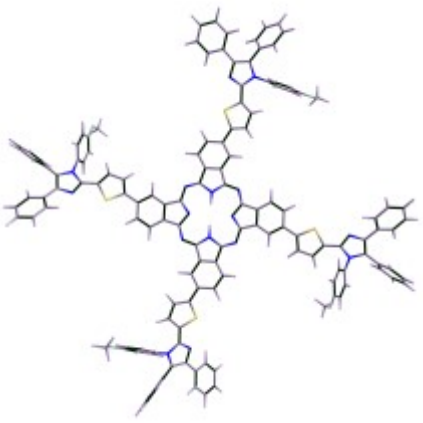	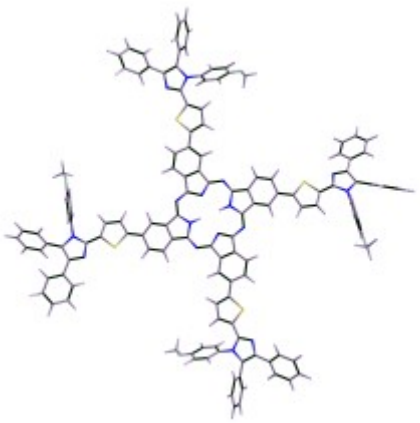
Zn-TIPc	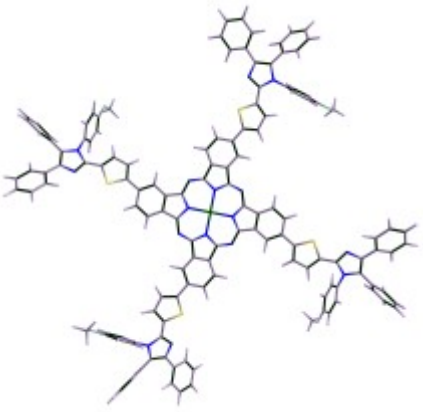	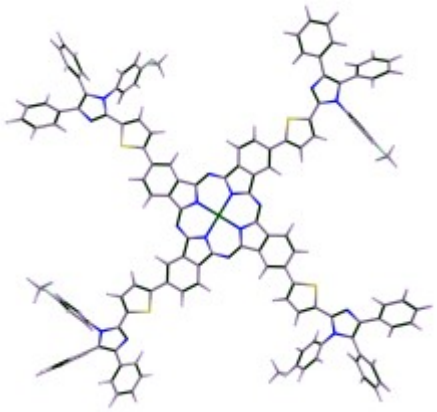
Cu-TIPc	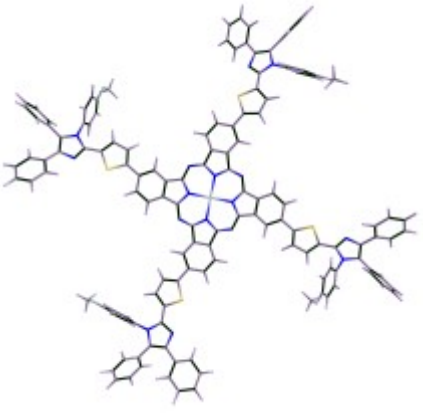	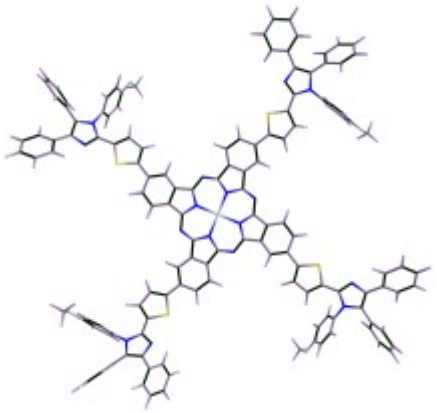

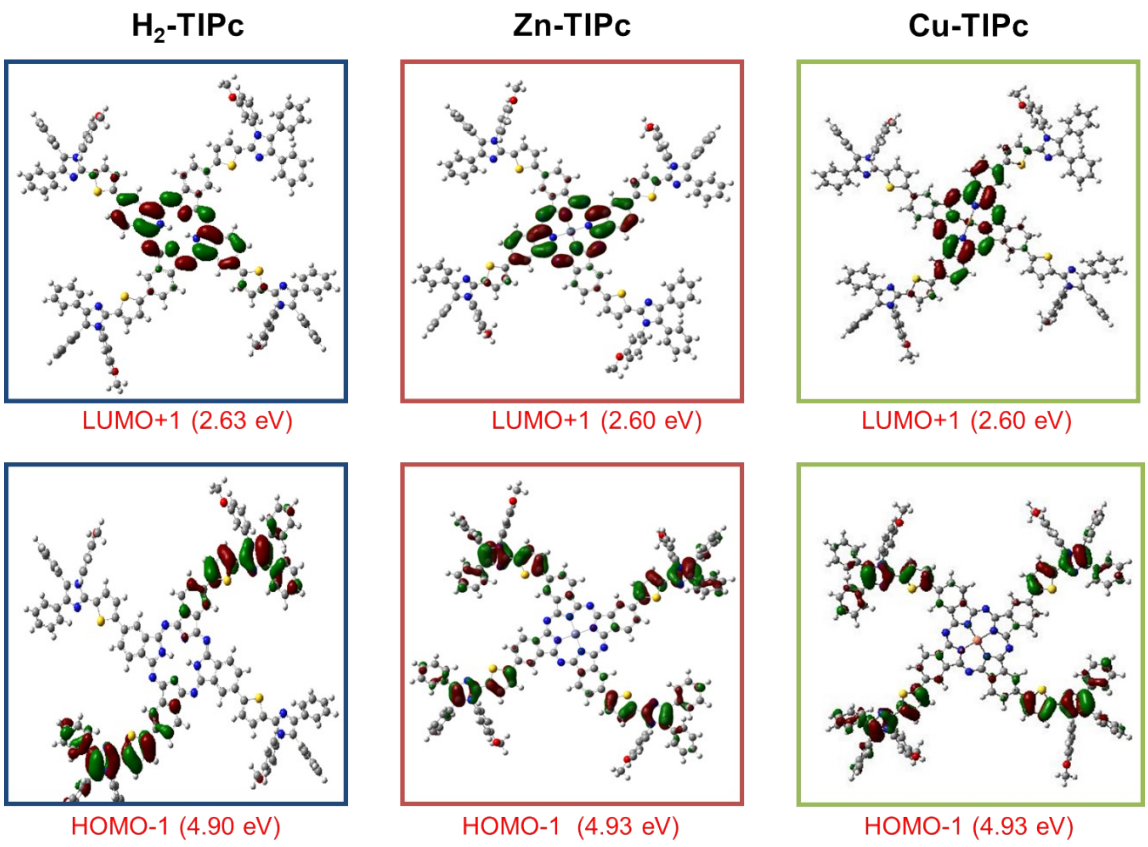

Fig. S3. Isodensity plots of the FMOs (HOMO-1 and LUMO+1) based on the B3LYP 6-31G(d,p) method for H_2-TIPc, Zn-TIPc and Cu-TIPc.

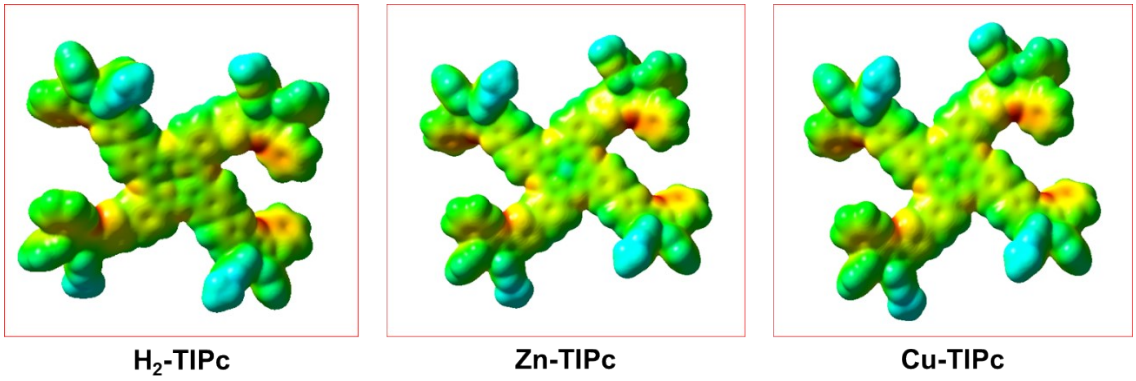

Fig. S4. ESP images of H_2-TIPc, Zn-TIPc and Cu-TIPc, obtained from DFT.

Transient absorption spectroscopy

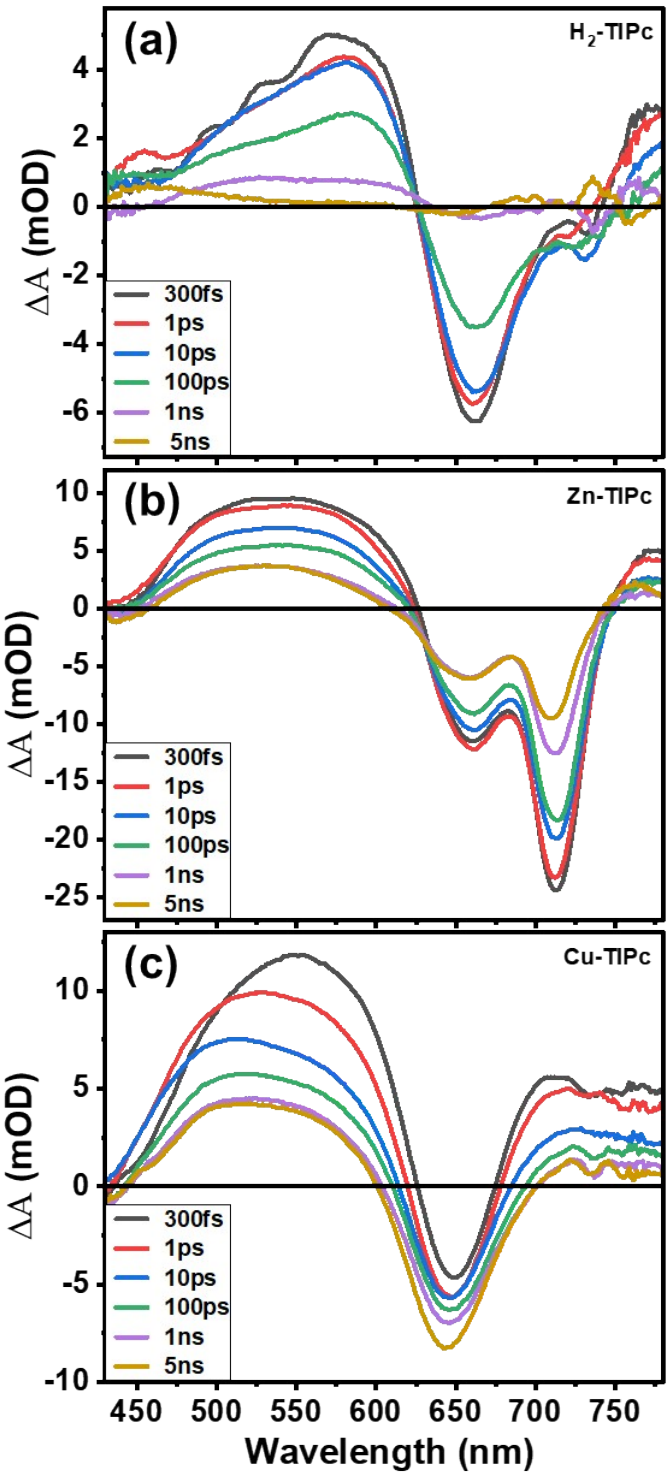

Fig. S5. fs-transient absorption spectra with different delay time collected with Soret band photoexcitation for (a) H_2-TIPc, (b) Zn-TIPc and (c) Cu-TIPc.

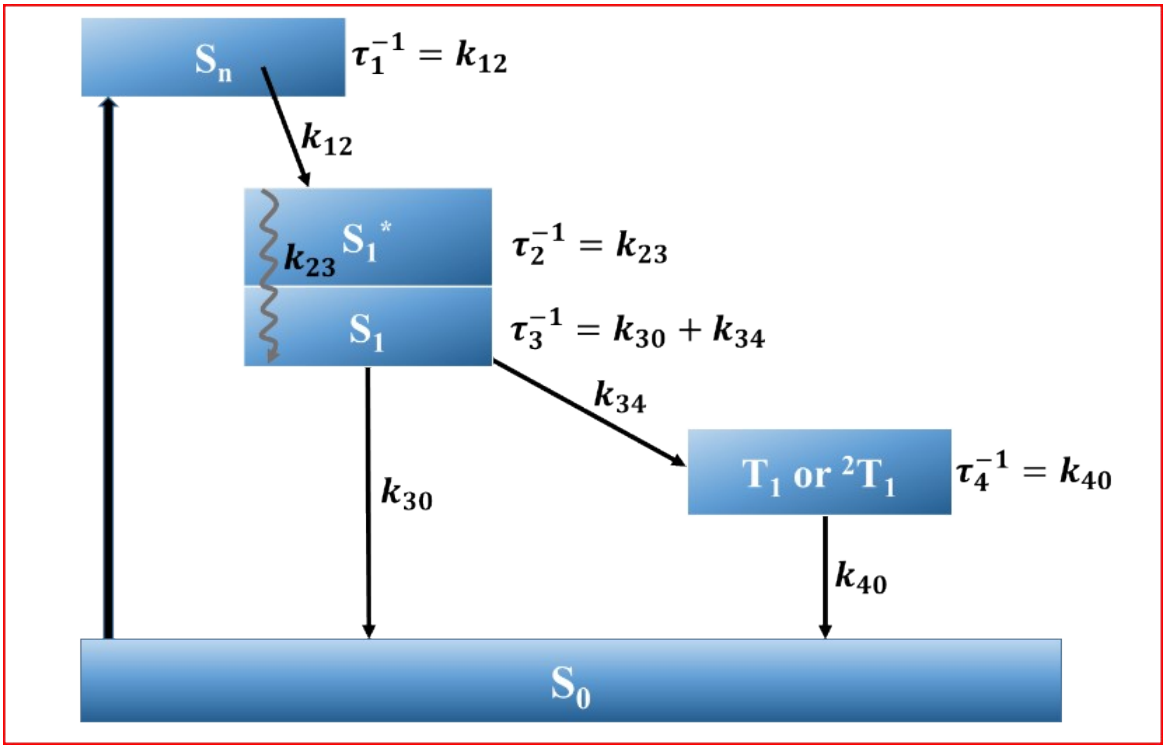

Fig. S6. Schematic of the photophysical model used in the target analysis of TAS data.

Z-scan

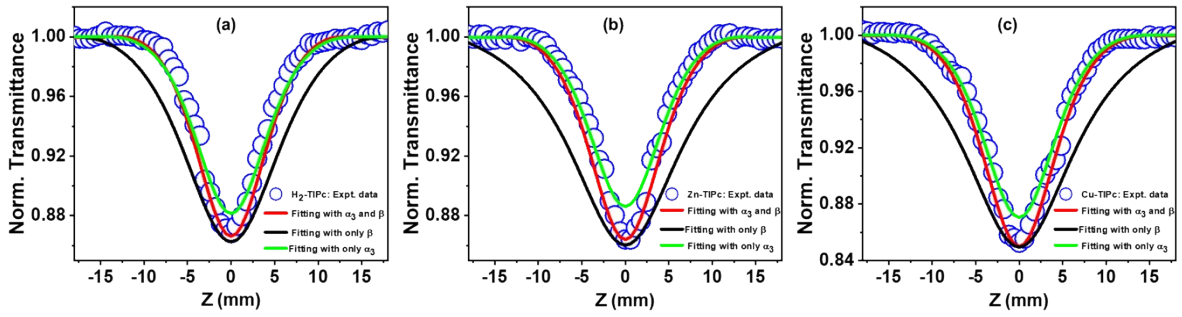

Fig. S7. OA Z-scan data theoretically fitted with β, α_3 and combination of $\beta$and α_3 for (a) H2-TIPc, (b) Zn-TIPc and (c) Cu-TIPc.

Equation for calculating 2PA cross-section [1]:

$$\sigma_{2PA} = \frac{\hbar\omega}{N}\beta \quad \text{(S1)}$$

Equation for calculating 3PA cross-section[1]:

$$\sigma_{3PA} = \frac{(\hbar\omega)^2}{N}\alpha_3 \quad \text{(S2)}$$

where N is the number density of molecule in solution samples, α_3 is the 3PA coefficient.

Equation for theoretical fit of closed aperture Z-scan data[2]:

$$T_{CA}(x) = 1 + \frac{4x\Delta\Phi}{(1+x^2)(9+x^2)} + \frac{4(3x^2-5)\Delta\Phi^2}{(1+x^2)(9+x^2)(25+x^2)} + \frac{}{(1} \quad \text{(S3)}$$

Here, $T_{CA}(x)$ is the normalised transmittance, $x = -z/z_0$, z is the sample's longitudinal distance from the focus point (z=0), z_0 is the Raleigh range and $\Delta\Phi$ is the on-axis nonlinear phase shift.

The relationship[3] that was utilised to determine $\langle\gamma\rangle$:

$$\langle\gamma\rangle = \frac{\chi^{(3)}}{NL^4}, \quad \text{(S4)}$$

where $\chi^{(3)}$ is the third-order nonlinear susceptibility, N is the number density of molecule in solution samples, and the local field factor is $L = \frac{n_0^2+2}{3}$.

Table S3

Comparison the values of obtained second hyperpolarizability with the prior reports.

Compound	Laser parameters (used method)	$\gamma(esu)$	References
H_2-TIPc, Zn-TIPc, Cu-TIPc	~70 fs, 800 nm (Z-scan)	(2.34-3.61)×10^{-30}	Present work
Phthalocyanine, ZnPc	ns laser, 532 nm, 10 Hz	2.97×10^{-31}	4

Th-Fb, Th-Cu and Th-Zn	~70 fs, 800 nm (Z-scan)	1.23-2.42×10^{-31}	5
Quinoxalines	~70 fs, 800 nm (degenerate four wave mixing (DFWM))	~10^{-31}	6
uGFPc	~70 fs, 800 nm (Z-scan)	(2.17 - 6.07) × 10^{-33}	2
Orthogonal pyrrolotetrathiafulvalene derivatives (S1, S2, S3)	30 ps, 532 nm (Z-scan)	~10^{-31}	7
NLOphoric mono-azo dyes	(DFT, Solvatochromism)	~10^{-33}, ~10^{-34}, ~10^{-35}	8
Croconate dyes	100 fs, 800 nm (DFWM)	-2.4 to -5.3×10^{-32}	9
Squaraine Dyes	210 fs and 3 ps; 696 and 710 nm (DFWM)	~8 ×10^{-32}	10
Methyl orange dyes (azo dyes)	(Monte Carlo/DFT)	~10^{-34}	11
Azo dye	5 ns, 532 nm (Z-scan)	~10^{-35}	12
HMB	(Z-scan)	0.5×10^{-35}	13

References

1. S. V. Rao, K. N. Krishnakanth, C. Indumathi and T. S. Girisun, in *Handbook of Laser Technology and Applications*, CRC Press, 2021, pp. 255-287.
2. M. S. Ahmed, C. Biswas, D. Banerjee, P. Chetti, J.-S. Yang, V. R. Soma and S. S. K. Raavi, Femtosecond Third-Order Non-Linear Optical Properties of Unconstrained Green Fluorescence Protein Chromophores, *Frontiers in Physics*, 2022, 549.
3. C. Biswas, N. K. Katturi, N. Duvva, L. Giribabu, V. R. Soma and S. S. K. Raavi, Multistep electron injection dynamics and optical nonlinearity investigations of π-extended thioalkyl-substituted tetrathiafulvalene sensitizers, *The Journal of Physical Chemistry C*, 2020, **124**, 24039-24051.
4. J. Britton, A. G. Martynov, D. O. Oluwole, Y. G. Gorbunova, A. Y. Tsivadze and T. Nyokong, Improvement of nonlinear optical properties of phthalocyanine bearing diethyleneglycole chains: Influence of symmetry lowering vs. heavy atom effect, *Journal of Porphyrins and Phthalocyanines*, 2016, **20**, 1296-1305.

5. M. S. Ahmed, C. Biswas, B. Bhavani, S. Prasanthkumar, D. Banerjee, V. Kumar, P. Chetti, L. Giribabu, V. R. Soma and S. S. K. Raavi, Metalated porphyrin-napthalimide based donor-acceptor systems with long-lived triplet states and effective three-photon absorption, *Journal of Photochemistry and Photobiology A: Chemistry*, 2023, **435**, 114324.
6. C. Biswas, K. Krishnakanth, J. Lade, A. Chaskar, A. Tripathi, P. Chetti, V. R. Soma and S. S. K. Raavi, Linear and femtosecond nonlinear optical properties of soluble pyrrolo [1, 2-a] quinoxalines, *Chemical Physics Letters*, 2019, **730**, 638-642.
7. K. Iliopoulos, R. Czaplicki, H. El Ouazzani, J.-Y. Balandier, M. Chas, S. Goeb, M. Sallé, D. Gindre and B. Sahraoui, Physical origin of the third order nonlinear optical response of orthogonal pyrrolo-tetrathiafulvalene derivatives, *Applied physics letters*, 2010, **97**, 101104.
8. U. Warde and N. Sekar, NLOphoric mono-azo dyes with negative solvatochromism and in-built ESIPT unit from ethyl 1, 3-dihydroxy-2-naphthoate: Estimation of excited state dipole moment and pH study, *Dyes and Pigments*, 2017, **137**, 384-394.
9. C. Prabhakar, K. Yesudas, K. Bhanuprakash, V. J. Rao, R. S. Santosh Kumar and D. N. Rao, Linear and nonlinear optical properties of mesoionic oxyallyl derivatives: enhanced non-resonant third order optical nonlinearity in croconate dyes, *The Journal of Physical Chemistry C*, 2008, **112**, 13272-13280.
10. K. Tran, G. W. Scott, D. J. Funk and D. S. Moore, Resonantly enhanced, Degenerate four-wave mixing measurement of the cubic molecular hyperpolarizability of squaraine dyes at 700 nm, *The Journal of Physical Chemistry*, 1996, **100**, 11863-11869.
11. V. Manzoni, L. Modesto-Costa, J. Del Nero, T. Andrade-Filho and R. Gester, Strong enhancement of NLO response of methyl orange dyes through solvent effects: A sequential Monte Carlo/DFT investigation, *Optical Materials*, 2019, **94**, 152-159.
12. M. Sreenath, I. H. Joe and V. Rastogi, Experimental and theoretical investigation of third-order nonlinear optical properties of azo dye 1-(2, 5-Dimethoxy-phenylazo)-naphthalen-2-ol by Z-scan technique and quantum chemical computations, *Dyes and Pigments*, 2018, **157**, 163-178.
13. D. Jayareshmi, H. M. Robert and D. Aruldhas, Elucidation of the structure, spectroscopic techniques and quantum chemical investigations on nonlinear optical material 2-hydroxy-5-methylbenzaldehyde, *Journal of Molecular Structure*, 2021, **1238**, 130426.